Title: Particle Size Distribution Reconstruction: The Moment Surface Method

Authors: Kieran Hutton [a], Niall Mitchell [a], Patrick, J. Frawley [a].

Affiliation: [a] Solid State Pharmaceuticals Cluster (SSPC), Materials & Surface Science Institute, University of Limerick, Limerick, Ireland.

Keywords: Quadrature, Method of Moments, Dynamic, Population Balance Modelling, Particle Size Distribution, Reconstruction.

Abstract

Numerical simulation of typical chemical engineering processes, such as crystallisation, liquid-liquid extraction, milling and other multi-phase operations in which exist discrete and continuous phases are highly computationally intensive problems. For this reason numerical techniques, such as the Method of Moments (MOM) and Quadrature Method of Moments (QMOM), are utilised to improve the computational efficiency of these simulations. The downside to these approaches is that the simulations only produce the moments of the Particle Size Distribution (PSD), with the actual distribution not preserved. Knowledge of the PSD is very important for many industrial unit operations, particularly in dynamic multi-phase flows in chemical engineering where the composition of the discrete phase(s) evolves in time or space. For example, control of the PSD in crystallisation operations may be required to ensure more efficient downstream operations such as filtration and clarification. Several methods for the reconstruction of a distribution from its respective moments are available in the literature. Typically these techniques are quite computationally expensive. The novel technique presented in this paper involves the pre-calculation of the moments of a pre-defined 2-parameter Probability Density Function (PDF) for a range of values of each parameter. This pre-calculation results in moment surfaces where the surfaces are a function of the two defining parameters. The intersection of constant moment contour lines (termed moment iso-lines) on these surfaces using simulation moment outputs results in the recovery of the defining parameters. Knowledge of the PDF and the total particle count or solids loading allows for the reconstruction of the full PSD. This technique proves to be very efficient which makes it ideal for the reconstruction of large numbers of distributions, for example in transient population balance models or model-based control algorithms, without the need for repeated application of optimisation algorithms.

1 Introduction

Numerical modelling of chemical engineering processes in the process and academic sectors has been receiving a renewed interest and importance in the last decade, due to the marked increase in computational power afforded by advances in electronics and computer technology as well as advances in numerical and computational techniques and algorithms. However, the simulation of these processes is still plagued by the massive computational requirements of full scale process modelling. There are three major issues associated with this computational work. The first is the issue of processing power or the number of computations that can be performed in a given length of time. The second concerns the amount of memory required for the processing of simulation data and finally, the storage and access to the computed outputs. For particulate processes, such as crystallisation or aerosol systems, the PSD must, ideally, be stored at each time step of the simulation.

In order to minimise the computational requirements of these process models, a number of mathematical techniques have been utilised to either reduce the number of computations or outputs, and/or reduce the amount of memory required to perform these simulations. These techniques include the Method of Moments (MOM), first proposed by Randolph & Larson [1] and the Quadrature Method of Moments (QMOM) [2,3], which can significantly reduce the computational costs of numerical simulations of multiphase processes. These techniques involve the tracking of the moments of the distribution in place of the actual PSD. This simplification eliminates the need to track each particle class which is very computationally expensive should high accuracy be required, as high accuracy translates to a high number of particle size classes. However, the main downfall of these methods is that the PSD remains unknown during the course of the simulation. QMOM is a widely used technique for coupling population balance modelling with Computational Fluid Dynamics (CFD) where the number of additional transport equations to be solved must be kept to a minimum in order to maximise computational efficiency. Typical applications include tracking evolving particle, droplet or bubble phase distributions in engineering unit operations.

The PSD generally constitutes a key process result which may be used to gauge the performance of the process. The size and size distribution of particles in a particulate process, such as milling or crystallisation is particularly important for several reasons. These properties heavily influence the efficiency of downstream processes, such as filtration and

centrifugation, where a small product size can significantly increase processing time. Product particles may need to be dissolved for subsequent use, with a broad size range resulting in a wide variation in the time required for dissolution of product crystals [4]. This may become a key process driver when issues such as the bioavailability of pharmaceutical compounds becomes important. For these reasons it is vital to be able to control and predict the PSD in these processes.

It is therefore necessary to reconstruct the PSD from the computed moments. The reconstruction of a PSD from its corresponding moments is a long studied problem, first considered by Von Smoluchowski [5] and is also known at the "finite-moment problem"[6]. Since then a number of reconstruction techniques have been proposed. A reconstruction technique involving the maximization of the entropy of the distribution has been proposed by some authors [7-9]. However, this technique requires significant computational effort, particularly for systems with evolving PSDs. An alternative technique was developed by Baldyga and Orciuch [10] to evaluate the PSDs of a Barium Sulphate ($BaSO_4$) precipitation system. This method is based on *a priori* knowledge of the mean and variance of the distribution, with three potential models suggested by the authors. This technique is also highly computationally intensive and may be prohibitively time consuming for simulations with a large number of time steps.

An indication of the mean particle size can be evaluated from the ratio of two moments, using $\mu = m_{k+1}/m_k$. However, no unified technique for reconstruction of a complete distribution from a finite number of its moments is available in the literature. This is due to the fact that, mathematically, all the moments of a distribution up to infinity are required to achieve an accurate reconstruction [11]. It has also been shown that knowledge of all moments is insufficient to determine a function or PSD uniquely [12]. Simple *a priori* shapes for the distribution are commonly assumed, such as Log-Normal and Weibull, in order to reconstruct a function from a finite number of its moments. These approaches generally only utilise the first three moments of a distribution for their reconstruction, but can provide an efficient and accurate method for PSD reconstruction. These techniques are detailed and outlined for sample PSDs in a recent work by John et al. [11]. This publication also provides an overview of some of the available literature concerning PSD reconstruction techniques.

Recently, spline-based reconstruction techniques have been proposed by some authors [11,13]. Splines or piecewise polynomials are utilised in this technique to evaluate the shape of the function in discrete intervals of the distribution, with no assumptions made about the shape of the function to be reconstructed. The accuracy of the technique is highly dependent on the order of the splines and the number of moments utilised in the reconstruction [11]. An improvement to this method has been recently proposed, involving the use of an adaptive grid for the nodes of the distribution. The new method was found to show considerable improvements on the original method, particularly for non-smooth distributions [13].

A novel technique for reconstruction of a PSD from its respective moments will be outlined in the following section. This technique assumes an *a priori* distribution for the PSD to be reconstructed, but it is not limited to the first three moments of a distribution. The accuracy of the technique will be demonstrated using sample Weibull and Log-Normal distributions and the potential expansion of the method to cover more advanced functions will also be discussed.

2 Material & Methods

2.1 Novel PSD Reconstruction

A novel technique for reconstructing the PSD from the moments of the distribution will now be outlined. This technique can be used to reconstruct any 2-parameter distribution based on any two moments. Examples of possible functional forms of the 2-parameter PSD include the Weibull, Gamma, Gaussian and Log-Normal distributions. In the current work the Weibull and Log-Normal density functions are used as the working examples.

The Weibull and Log-Normal probability distributions are defined, respectively, as:

$$P(L) = \frac{n}{\delta^n} L^{n-1} \exp\left(-\left(\frac{L}{\delta} \right)^n \right) \tag{1}$$

$$P(L) = \frac{1}{L\sigma\sqrt{2\pi}} \exp\left(\frac{-\left(\ln(L) - \mu \right)^2}{2\sigma^2} \right) \tag{2}$$

Where *P(L)* is the continuous Probability Density Function (PDF). *L* is the particle diameter, *n* and δ are the distribution defining parameters for a Weibull distribution and μ and σ are the defining parameters for a Log-Normal distribution. Three sample Weibull distributions, shown in Figure 1, are employed to outline and demonstrate the accuracy of the reconstruction technique. Also, sample Log-Normal distributions, shown in Figure 2, will be reconstructed from its respective moments using this technique.

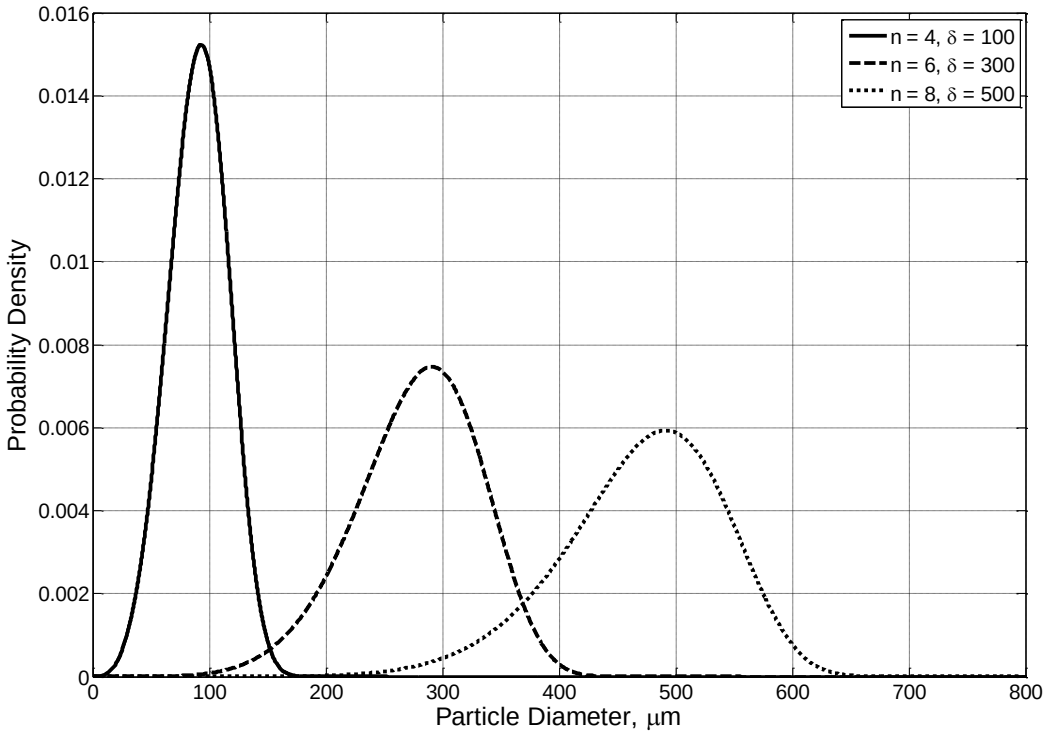

Figure 1. Sample Weibull Distributions.

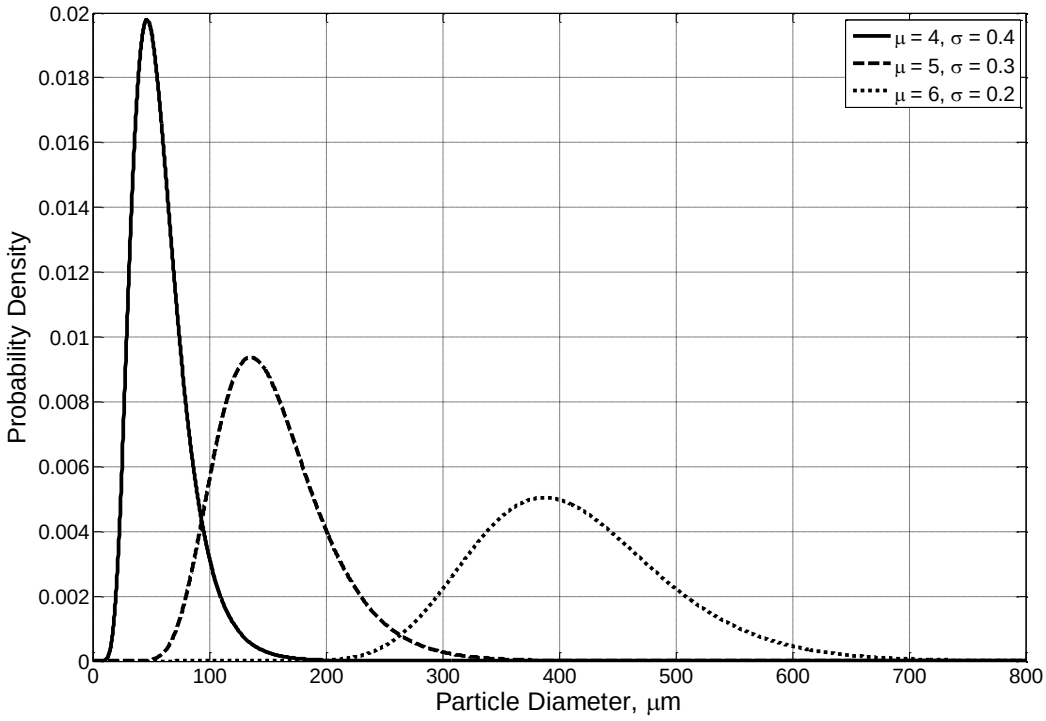

Figure 2. Sample Log-Normal Distributions.

2.2 Moment Surface Generation

In this technique a range of values of the distribution defining parameters are used to generate the number based moment surfaces. The extrema of these parameters are selected to encompass the values that could be encountered in the modelled system. A typical example of an extreme case would be one where the PDF assumes a very narrow range at very large values of particle size. The extrema are chosen so that the PDF covers the entire range of physically realisable distributions encountered in the modelled system. The ranges of n and δ used in the Weibull case were 2 – 8 and 10 - 500, respectively while the μ and σ used in the Log-Normal case are 0.01-6 and 0.01-2 respectively. The number based moments for the distribution are calculated as follows:

$$m_k = \int_0^\infty L^k P(L)\, dL \tag{3}$$

Where m_k are the number based moments. Using the above equation the number based moment surfaces can be generated for the k^{th} moment as a function of the two defining parameters.

The equation for a Weibull or Log-Normal moment surface may be given as

$$m_k(n,\delta) = \int_0^\infty \frac{n}{\delta^n} L^{k+n-1} \exp\left(-\left(\frac{L}{\delta}\right)^n\right) dL \tag{4}$$

$$m_k(\mu,\sigma) = \int_0^\infty \frac{L^{k-1}}{\sigma\sqrt{2\pi}} \exp\left(\frac{-\left(\ln(L)-\mu\right)^2}{2\sigma^2}\right) dL \tag{5}$$

The 0^{th} moment surfaces generated using this technique are not shown as they are simply flat surfaces spanning the $m_0 = 1$ plane.

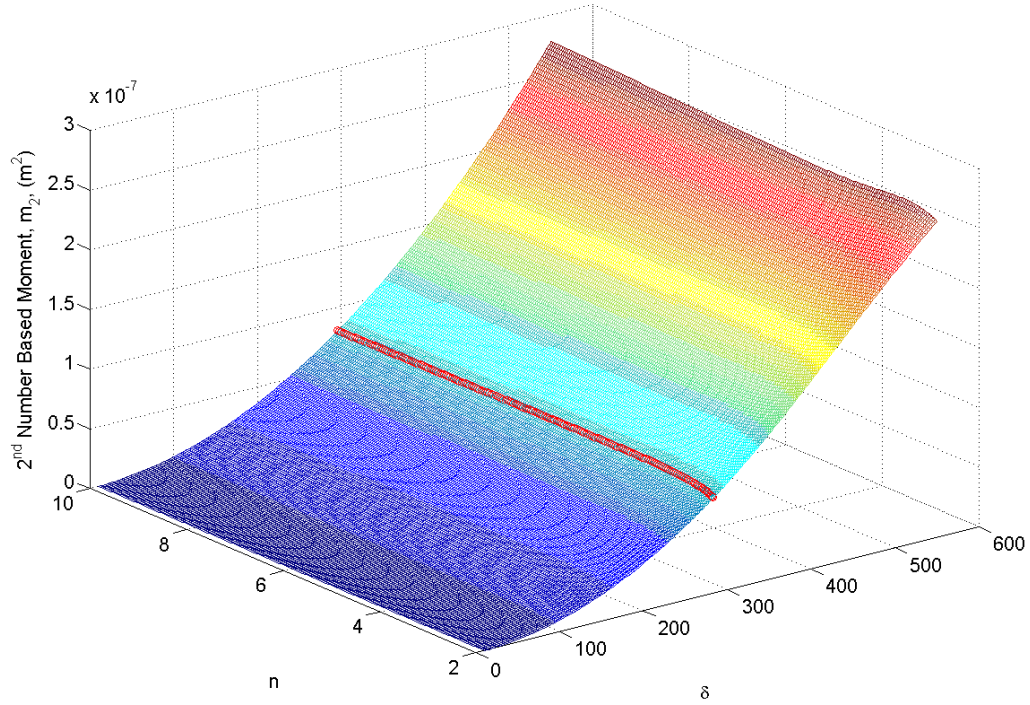

Figure 3. Second Moment, m_2, for the Weibull Distribution.

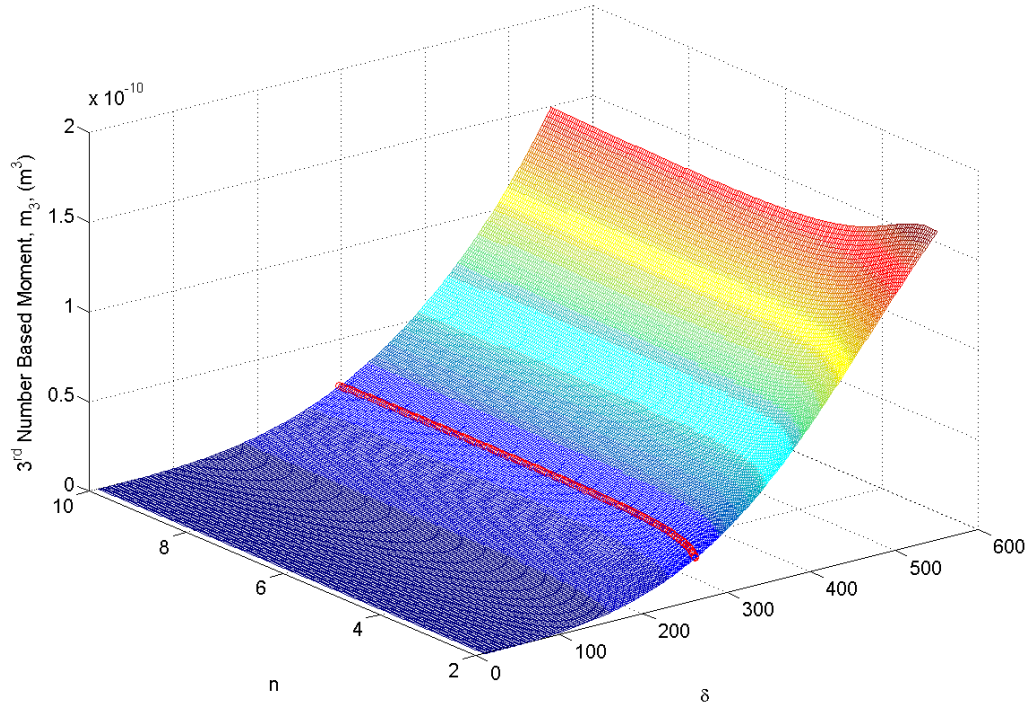

Figure 4. Third Moment, m_3, for the Weibull Distribution.

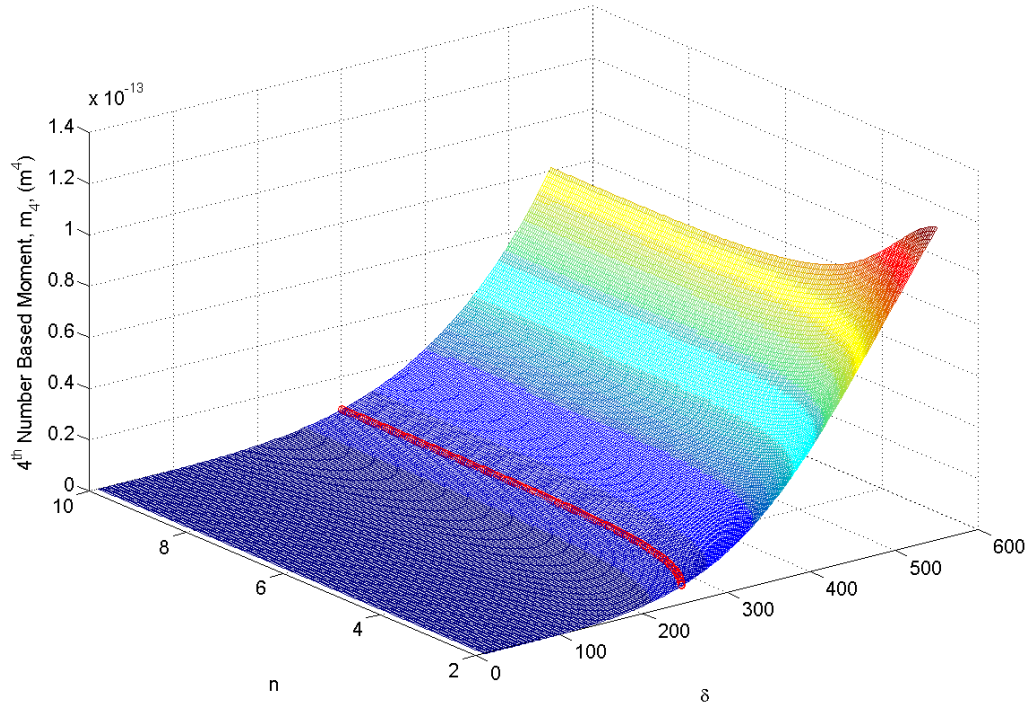

Figure 5. Fourth Moment, m_4, for the Weibull Distribution.

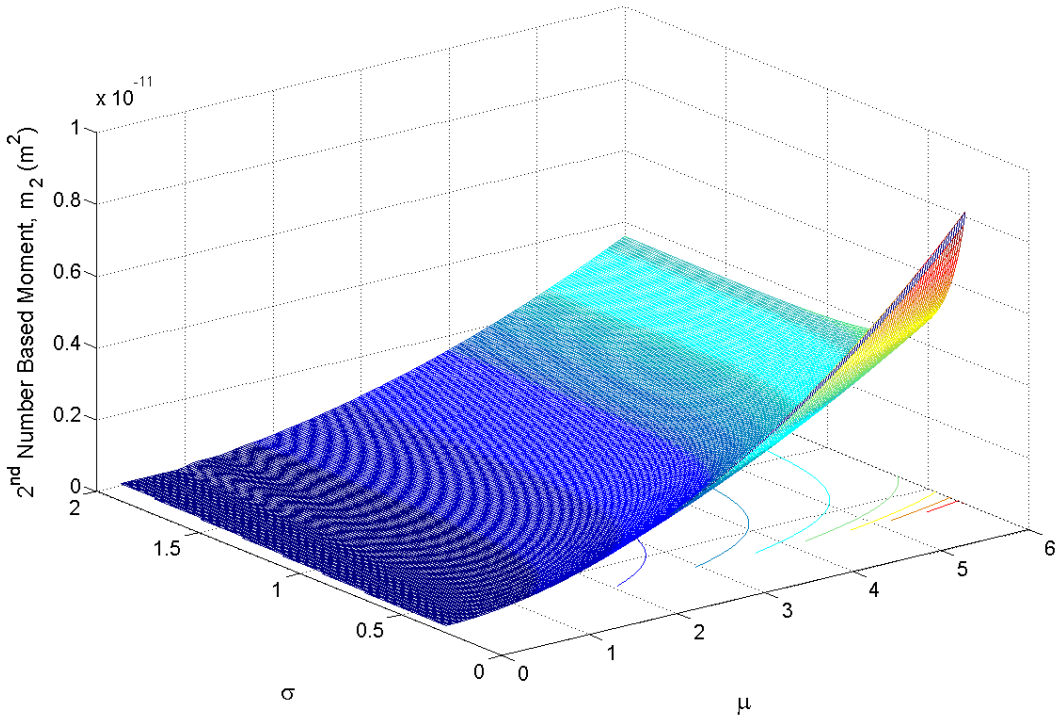

Figure 6. Second Moment, m_2, for the Log-Normal Distribution.

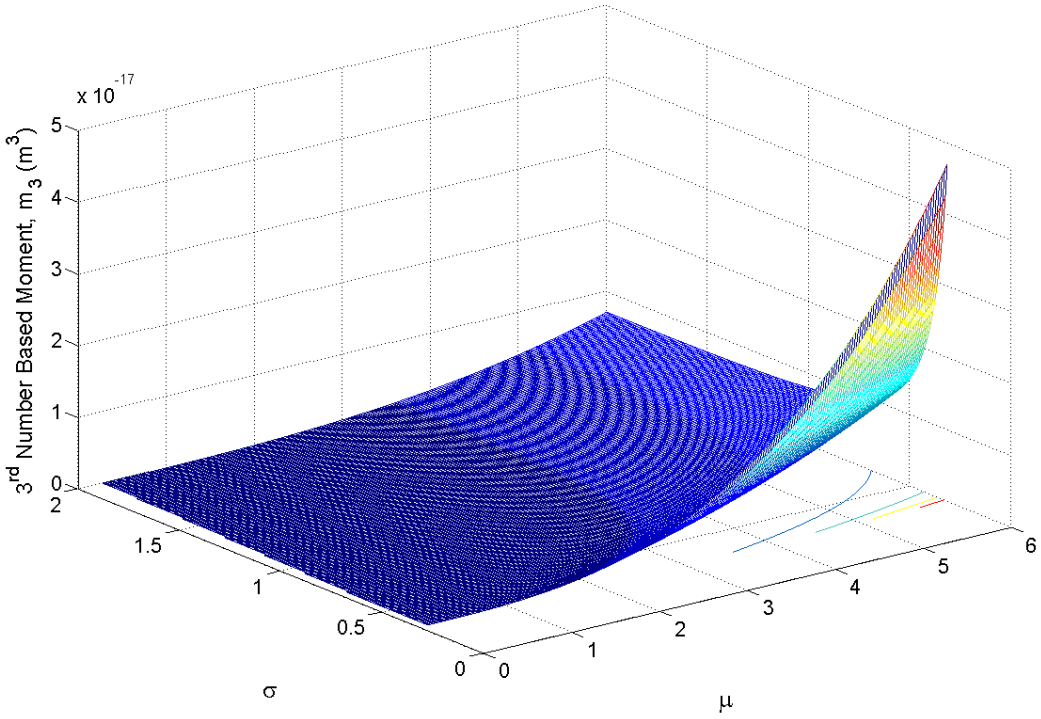

Figure 7. Third Moment, m_3, for the Log-Normal Distribution.

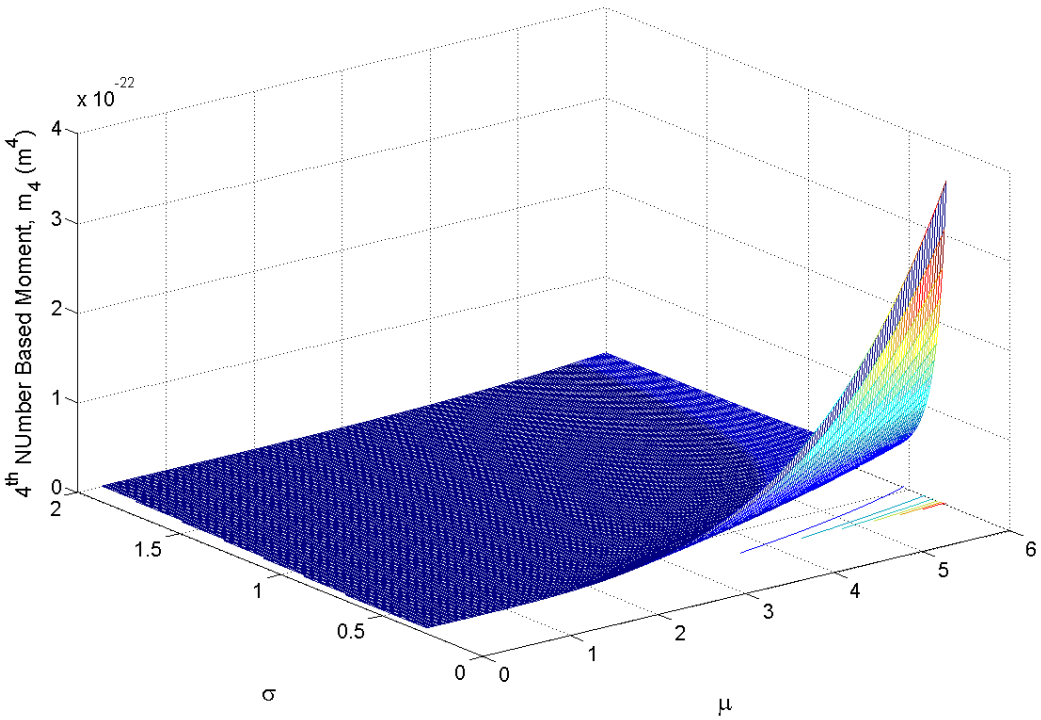

Figure 8. Fourth Moment, m_4, for the Log-Normal Distribution.

By plotting the moment surfaces (Figure 3 - Figure 8), it can be seen that each of the surfaces generated is unique within the set. The importance of this uniqueness will become clearer as the technique is discussed in more detail in the next section. The 2nd through 4th moments are given here as these are the moments used in the reconstruction. These moments are chosen with the aim of maintaining the accuracy of the Sauter and Volume Averaged mean particle diameter.

2.3 Moment Iso-lines

For this technique the moments (typically obtained from a method of moments' simulation) must be first normalised with respect to the 0^{th} moment. This results in the PSD's corresponding PDF. This is done as follows:

$$m_{k,n} = \frac{m_k}{m_0} \tag{6}$$

Where $m_{k,n}$ is the k^{th} normalised PSD moment which equates to the k^{th} moment of the PDF. To then extract the PDF, the simulated moments must be compared to the moment surfaces. For a given simulated moment, this value is compared to the corresponding moment surface. The points where the simulated moments are equal to the corresponding moment surface trace a line. This line has been termed the "moment iso-line". This iso-line may be likened to an iso-bar on a meteorological plot or an elevation contour line on a geographical map. For each output moment there exists one iso-line on the surface. For the Weibull distribution these iso-lines may be seen in Figure 3 - Figure 5 as the thick red line which spans the surface. The intersection of these moment iso-lines on a plot of n versus δ, for the Weibull distribution, reveals the values of n and δ that result in the best fit PDF for this pre-assumed functional form. The intersection point corresponds to the values of the defining parameters that satisfy the two imposed conditions, i.e. the values of the simulation output moments, namely m_2-m_4. It is at this intersection point that the simulated moments and the surface moments match and thus represent the values of the defining parameters which best define the shape and size of the distribution. These intersections may be seen in Figure 9. The intersection of these moment iso-lines on a plot of μ and σ also provides the best fit PDF for an assumed Log-Normal distribution. These intersection points are given in Table 4.

3 Results & Discussion

3.1 Individual Test Cases

In order to test the technique, a number of distributions have been selected. The details of these cases are shown below in Table 1. These are the same distributions as were presented in Figure 1 & Figure 2.

Case	*Distribution*	*n*	δ	μ	σ
1	Weibull	4	100	-	-
2	Weibull	6	300	-	-
3	Weibull	8	500	-	-
4	Log-Normal	-	-	3	0.5
5	Log-Normal	-	-	4	0.4
6	Log-Normal	-	-	5	0.3

Table 1. Test Cases used for validation of the technique.

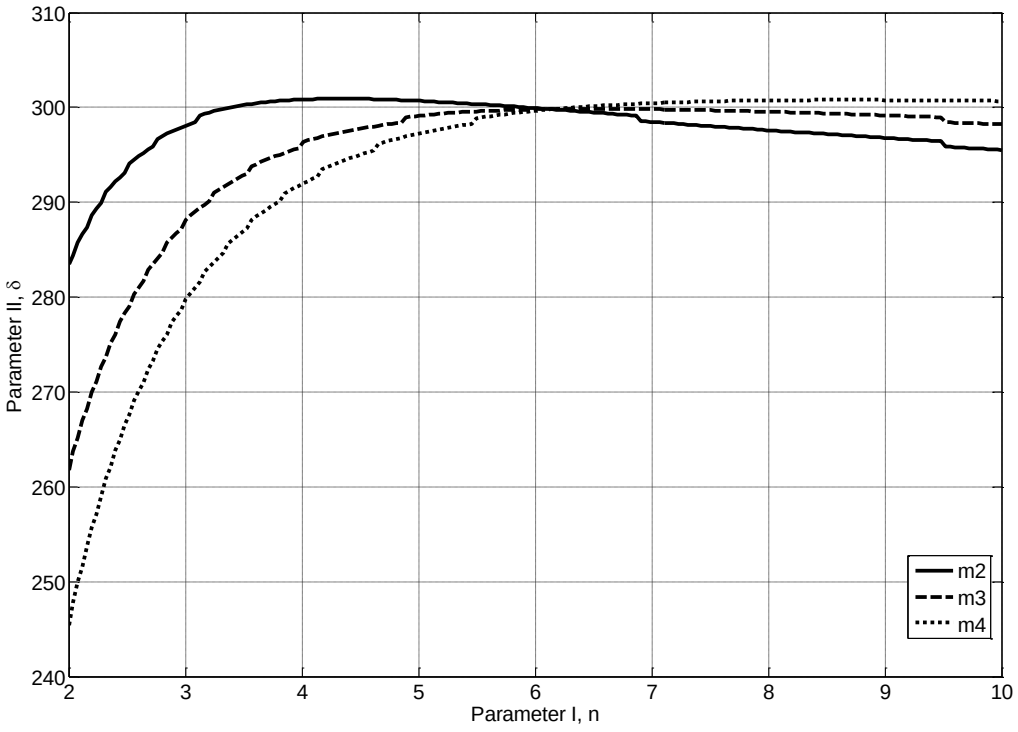

Figure 9. Intersection of Moment Iso-lines for Case 2.

As can be seen from Figure 9, the moment iso-lines from the 2^{nd}, 3^{rd} and 4^{th} Moment Surfaces, intersect at approximately the same location. The reason for the apparent stepped nature of the curves in Figure 9, is that the moment surfaces can only be generated for a finite number of points. This intersection point corresponds to the values of the defining parameters which satisfy the condition that the reconstructed distribution moments are the same as that of the simulation. If the equations for the moment surfaces were known, then the iso-lines would be perfectly smooth and would ideally intersect at exactly the same point. The intersection point of the moment iso-lines is also unique, as illustrated in Figure 9, where the curves can be seen to diverge away from the intersection point. In order to improve the accuracy of the obtained intersection point, the iso-line data is smoothed, using the following steps:

1. Locate the approximated intersection point, [6.143, 299.8]
2. Select five data points along each iso-line before and after the approximate intersection point.
3. Fit a quadratic equation to these data points.

   For Case 2 the following quadratics were obtained.

   $\mathbf{m_2}$: $3.4092\text{x}10^{-11}n^2 - 2.0149\text{x}10^{-08}n + 2.9788\text{x}10^{-06} = \delta$ (7a)

   $\mathbf{m_3}$: $1.4960\ \text{x}10^{-14}n^2 - 8.9235\text{x}10^{-12}n + 1.3313\text{x}10^{-09} = \delta$ (7b)

   $\mathbf{m_4}$: $6.0649\ \text{x}10^{-18}n^2 - 3.6471\text{x}10^{-15}n + 5.4856\text{x}10^{-13} = \delta$ (7c)
4. Find the intersections of these smoothing quadratics.

These intersection points provide values for the distribution defining parameters. These intersection points can be seen in Figure 10, a zoomed in view of the approximate intersection point.

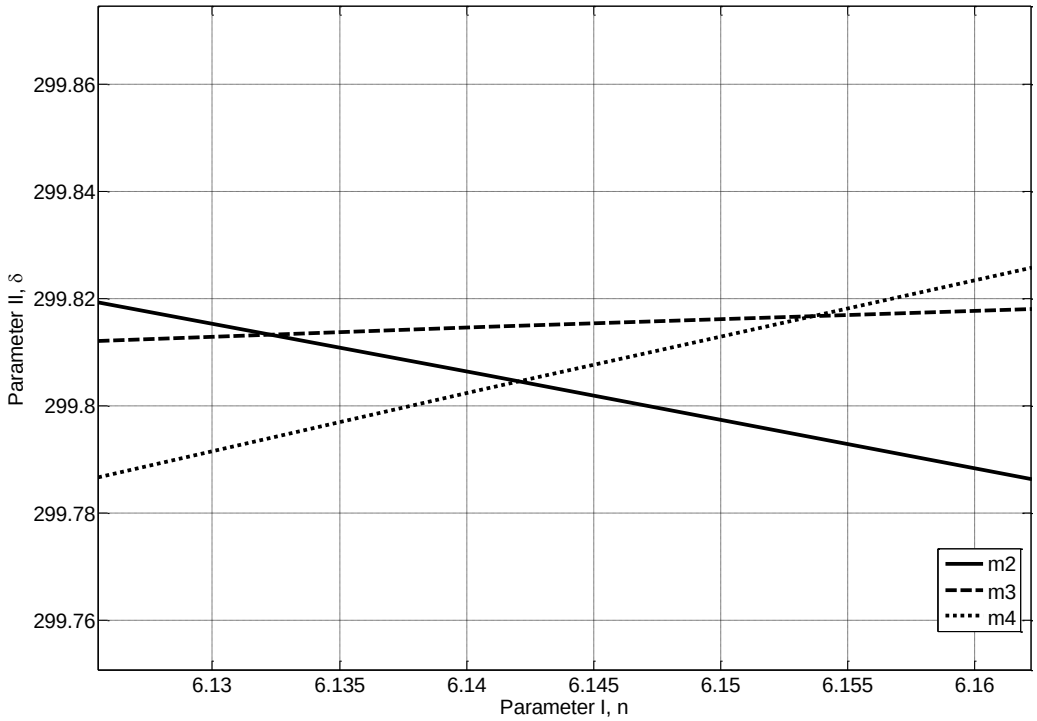

Figure 10. Close-up of the Intersection of Moment Iso-lines for Case 2.

As can be seen from Figure 10, the intersection points lie very close together. The values of the individual intersection points are reported in Table 2 below.

Case No.	***Source***	***n***	***δ***
2	Original Intersection	6	300
	$m_2 - m_3$	6.141	299.805
	$m_3 - m_4$	6.141	299.814
	$m_4 - m_2$	6.141	299.805

Table 2. Intersection Points Obtained for Case 2.

The intersection points for the other cases, including those of the Log-Normal cases, are provided below in Table 3 & Table 4.

Case No.	***Source***	***n***	***δ***
1	Original Intersection	4	100

	$m_2 - m_3$	4.492	99.490
	$m_3 - m_4$	4.412	99.442
	$m_4 - m_2$	4.412	99.494
3	Original	8	500
	Intersection		
	$m_2 - m_3$	8.110	499.978
	$m_3 - m_4$	8.110	499.990
	$m_4 - m_2$	8.110	499.978

Table 3. Intersection Points for Case 1 & Case 3.

The intersections for the Log-Normal distributions are determined in exactly the same way but using the corresponding moment surfaces.

Case No.	***Source***	μ	σ
4	Original	3	0.5
	Intersection		
	$m_2 - m_3$	2.9899	0.5076
	$m_3 - m_4$	3.0200	0.4834
	$m_4 - m_2$	3.0200	0.4772
5	Original	4	0.4
	Intersection		
	$m_2 - m_3$	4.0133	0.3798
	$m_3 - m_4$	4.0133	0.3854
	$m_4 - m_2$	4.0133	0.3798
6	Original	5	0.3
	Intersection		
	$m_2 - m_3$	5.0066	0.2883
	$m_3 - m_4$	5.0066	0.2862
	$m_4 - m_2$	5.0066	0.2862

Table 4. Intersection Points for Case 4 - Case 6.

3.2 Reconstructed PDFs

To prove the accuracy of the method, presented here are two examples of the reconstruction technique applied to Case 2 and Case 6.

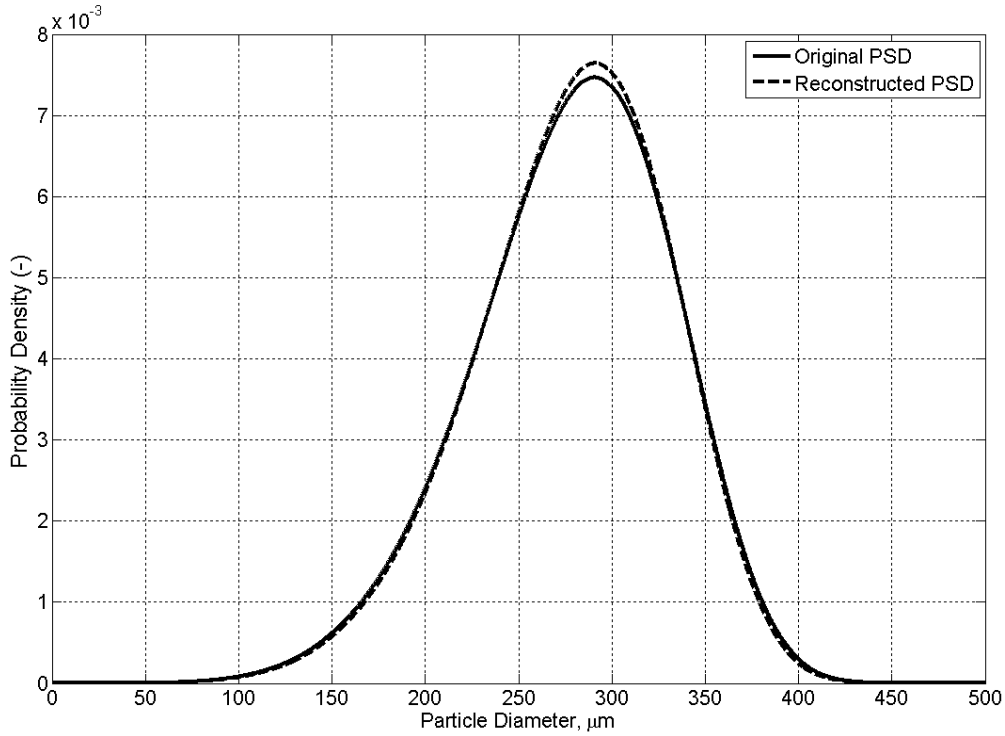

Figure 11. Original & Reconstructed PDF for Weibull Case 2, n=6, δ=300.

The reconstruction of Case 2, seen above in Figure 11, has been shown to be successful. The reconstructed PDF is almost identical to the original. There is a slight under-prediction of the lower end probabilities and a slight over prediction of the higher end probabilities. This error is insignificant enough to be neglected for this case. This insignificance can be seen below in the percentage errors in the moments, in Table 5.

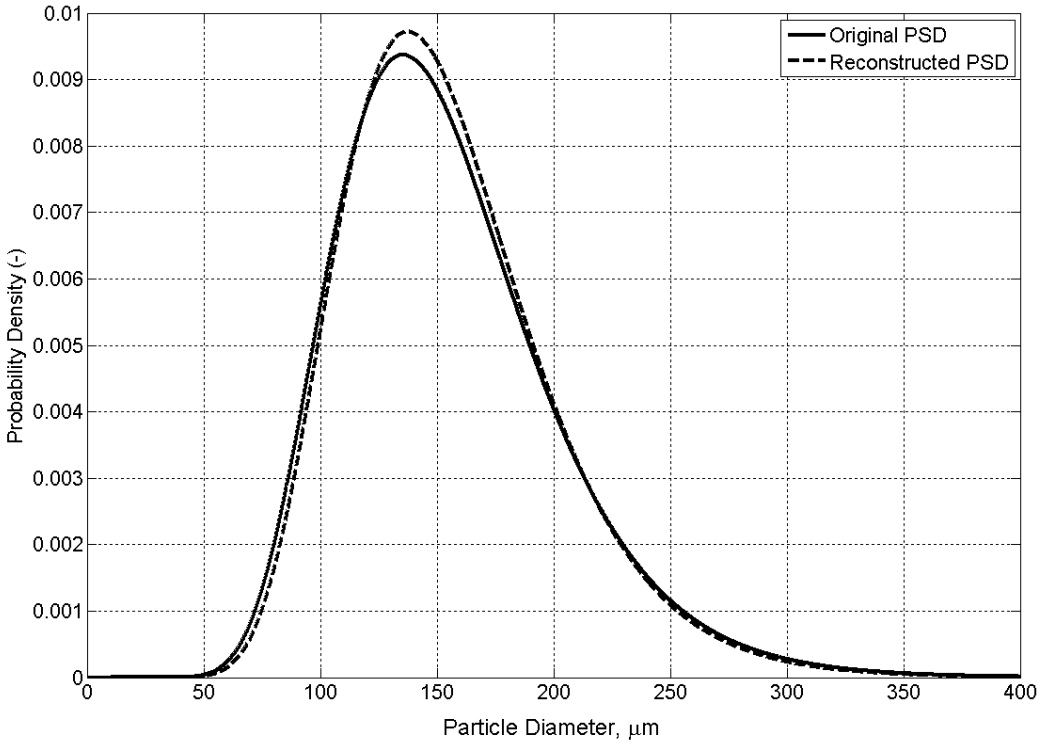

Figure 12. Original & Reconstructed PDF for Log Normal Case 6, μ=5, σ=0.3.

The reconstruction of the PDF for Case 6, seen above in Figure 12, has also been a success. The reconstructed PDF is very similar to the original, with similar under/over predictions of the lower/higher probabilities to Case 2 above. Again, these errors are small enough to be considered negligible. The insignificance of this error can be seen below in the percentage errors in the moments, in Table 5.

3.3 Reconstructed PDF Moment's % Error

Table 5 outlines the percentage error of the moments of the reconstructed PDF versus those of the original. It may be seen that the error in the moments increases with increasing order. This trend is to be expected due to the power-law dependence of the moments on the particle diameter. For engineering purposes the highest order moment of interest is the fourth moment. The maximum error in the 4th moment for these cases is 8.689% for Case 4.

Case	m_0	m_1	m_2	m_3	m_4	m_5
-	**%**	**%**	**%**	**%**	**%**	**%**
1	0	-0.157	1.074	3.250	6.087	9.389

2	0	-0.063	0.026	0.231	0.527	0.900
3	0	-0.062	-0.069	-0.033	0.040	0.144
4	0	0.823	2.034	4.457	8.689	13.606
5	0	-0.613	0.216	2.451	5.998	10.709
6	0	-0.276	0.217	1.469	3.450	6.115

Table 5. Reconstructed Moments % Error.

3.4 Dynamic Simulation Example

Presented here are the results of a 1-dimensional Quadrature Method of Moments simulation of a paracetamol crystallisation system involving growth and agglomeration. This simulation was run for a total of 2hrs (7200s). The kinetics for growth were obtained from the work of Mitchell et al [14]. A constant agglomeration kernel of 10^{-14} was used to introduce a skewing of the distribution. This skewing would not be present in a pure size-independent growth system. The aim of this inclusion of agglomeration is to demonstrate the ability of the method to track changes in shape as well as position of the evolving PSD. Once the PDF is known, it may be scaled back to the PSD using either the total particle count or the solids loading.
For a solids loading of 0.084 kg solids/kg mixture, the simulation was performed with the initial moments of the PDF set as:

Moment Number	***Value***	***Units***
0	$1.000000 \times 10^{+00}$	(-)
1	9.124554×10^{-05}	m
2	8.857162×10^{-09}	m^2
3	9.029898×10^{-13}	m^3
4	9.586704×10^{-17}	m^4
5	1.053468×10^{-20}	m^5

Table 6. Initial PDF Moments used in the sample QMOM simulation.

The relative changes in the moments of the simulation are plotted below in Figure 13. The relative change is defined as follows.

$$m_{k,rel}(t) = \frac{m_k(t)}{m_k(0)} \tag{8}$$

Where $m_k(t)$ and $m_k(0)$ are the k^{th} moment at time, t and initially respectively.

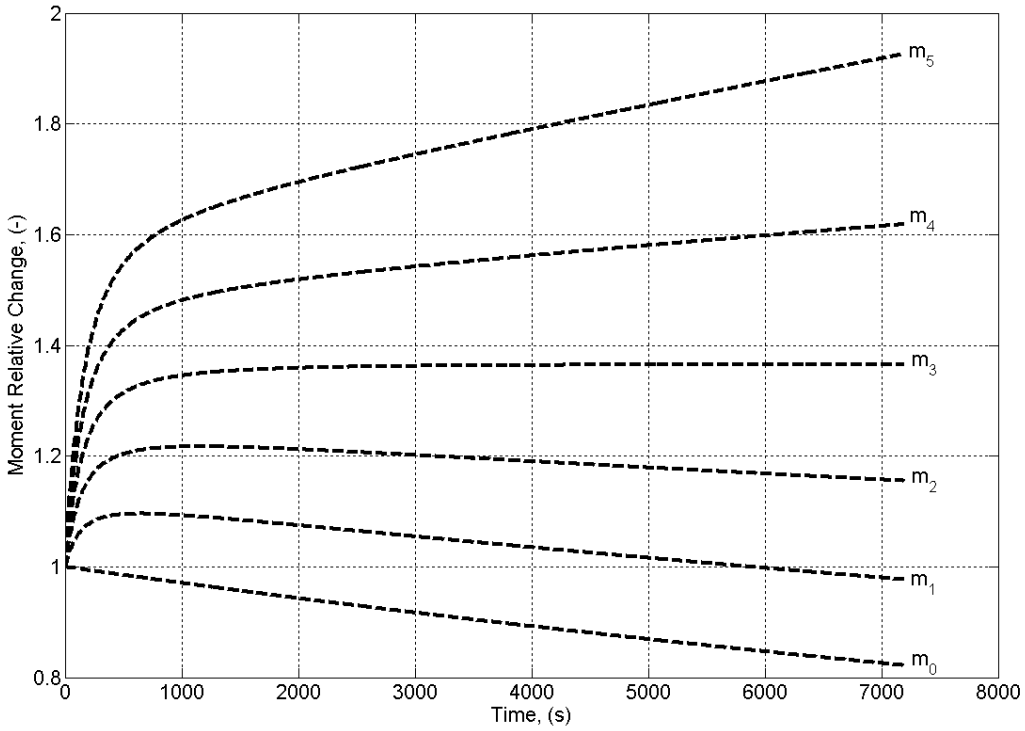

Figure 13. Relative Change in Moments in the Dynamic QMOM Simulation.

As can be seen from Figure 13 the 0^{th} moment was seen to decrease from the start. This trend is indicative of particle agglomeration. Moments 1 & 2 can be seen to increase initially due to growth and as the process advances, agglomeration becomes the dominant mechanism. The 3^{rd} moment plateaus, which is what would be expected from such a system. Moments 4 & 5 increase throughout the simulation, which is as a result of the combined effects of growth and agglomeration.

The absolute values of these moments were used as inputs to the reconstruction algorithm and the following particle size distributions were obtained.

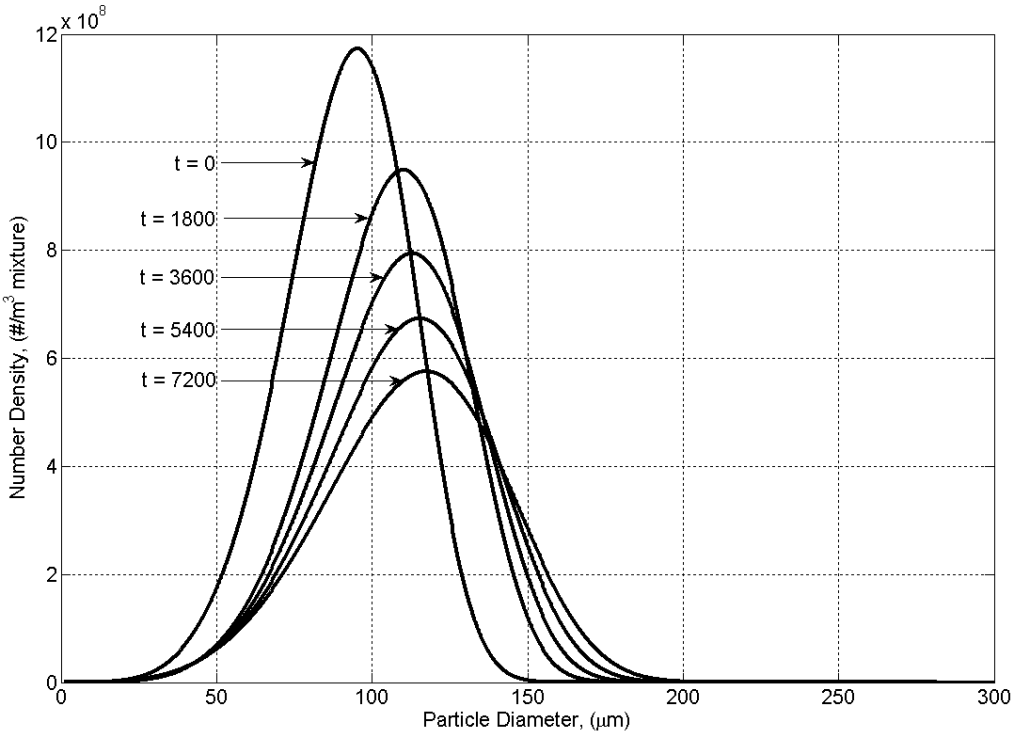

Figure 14. Dynamic QMOM Simulation Reconstructed PSDs.

The plots seen in Figure 14 were obtained from using the reconstruction algorithm described. It can be seen, as would be expected from a growth-agglomeration system, that the PSD experiences both a right hand shift and a skewing towards the larger particle sizes. This skewing is as a result of the repeated formation of single large particles from the collision and successful agglomeration of two smaller particles. It may be concluded, based on this and the previous examples that this technique provides an efficient and accurate reconstruction of PSDs from their respective moments, with the provision that the PSD may be taken to have a specific functional form.

3.5 Expandability

The technique outlined above is limited to distributions that can be described by 2-parameter PDF's. This method can potentially be expanded to 3-parameter PDF's. The difference between the 2- parameter and 3-parameter reconstruction techniques is that the 3-parameter PDF reconstruction would require 3 moments. The 3- parameter technique would result in 4-dimensional moment hyper-surfaces for each of the moments. Instead of the moment iso-lines generated for 2-parameter PDF's, a series of moment iso-surfaces would be generated for a given moment value. The intersection point of the three moment surfaces

would correspond to the best-fit values for the three parameters, defining the distribution. Use of this technique for 3 parameter PDF reconstruction may prove to be quite computationally expensive although an efficient solution to this expansion problem is currently under investigation.

Application to bimodal systems is also possible, where the simulations track 2 sets of low order moments rather than using a single set of moments where high order moments may prove to be unstable/inaccurate. This method would involve a mass weighted combination of the two reconstructed distributions.

4 Conclusions

In this study, a new technique was outlined which can efficiently and accurately reconstruct a full PDF from any two moments, assuming an *a priori* functional form for the distribution. The intersection of the moment iso-lines was found to produce the best-fit parameters for a given set of moments. For systems modelled by moment methods, such as crystallisation, whose distribution does not vary significantly from one particular functional form, this technique provides a simple and effective solution to the closure problem associated with the moment methods. For example, in Computational Fluid Dynamics simulations where QMOM is used to track the discrete phase, the PSD at any point or time may be quickly reconstructed from the moments. This technique avoids the need to repeatedly apply optimisation algorithms in order to find the defining parameters which can prove to be quite computationally demanding.

Sample PSD reconstructions have been outlined as well as PSDs from a dynamic QMOM simulation showing how this technique can quickly (~0.4s per PSD) and accurately return the PSDs while conserving the underlying moments. The potential expansion of this technique to reconstruct 3-parameter PDF's has also been outlined.

5 References

[1] A.D. Randolph, M.A. Larson, Theory of Particulate Processes; Academic Press, Inc.: London, 1988.

[2] D.L. Marchisio, R.D. Vigil, R.O. Fox, Quadrature method of moments for aggregation–

breakage processes, Journal of Colloid and Interface Science. 258 (2003) 322-334.
[3] R. McGraw, Description of Aerosol Dynamics by the Quadrature Method of Moments, Aerosol Science & Technology, 27(2) (1997) 255-265.
[4] A.S. Myerson, Handbook of Industrial Crystallization, 2nd Ed., Butterworth-Heinemann: Boston, 2002.
[5] M. Von Smoluchowski, Versuch einer mathematischen Theorie der Koagulationskinetik kolloider Losungen, Zeitschrift fur Physikalische Chemie. 92 (1917) 129-168.
[6] P. Chebyshev, Sur les Valuers Limites des Intégrales, Oeuvres, New York, 1961.
[7] S.B. Pope, A rational method of determining probability distributions in turbulent reacting flows, Journal of Non-Equilibrium Thermodynamics. 4 (1979) 309-320.
[8] K. Bandyopadhyay, A.K. Bhattacharya, P. Biswas, D.A. Drabold, Maximum entropy and the problem of moments: A stable algorithm, Physical Review 71 (2005) 057701/1-057701/4.
[9] J. Sanyal, D.L. Marchisio, R.O. Fox, K. Dhanasekharan, On the comparison between population balance models for CFD simulation of bubble columns, Industrial Engineering Chemistry Research. 44 (2005) 5063-5072.
[10] J. Baldyga, W. Orciuch, Closure Method for Precipitation in Inhomogeneous Turbulence, Industrial Crystallization. 1 (1999) 1-12.
[11] V. John, I. Angelov, A.A. Öncül, D. Thévenin, Towards the Optimal Reconstruction of a Distribution from its
Moments, Chemical Engineering Science. 62 (2007) 2890-2904.
[12] R. McGraw, S. Nemesure, S.E. Schwartz, Properties and evolution of aerosols with size distributions having identical moments, Journal of Aerosol Science. 29(7) (1998) 761-772.
[13] L.G.M. De Souza, G. Janiga, V. John, D. Thévenin, Reconstruction of a distribution from a finite number of moments with an adaptive spline-based algorithm, Chemical Engineering Science, 65 (2010) 2741-2750.
[14] N.A. Mitchell, C.T. Ó'Ciardhá, P.J. Frawley, Estimation of the growth kinetics for the cooling crystallisation of paracetamol and ethanol solutions, Journal of Crystal Growth, Vol 328, Issue 1, 39-49.